Biochimica et Biophysica Acta 1838 (2014) 2326–2330

Contents lists available at ScienceDirect

Biochimica et Biophysica Acta

journal homepage: www.elsevier.com/locate/bbamem

Strong dimerization of wild-type ErbB2/Neu transmembrane domain and the oncogenic Val664Glu mutant in mammalian plasma membranes ☆

Jesse Placone, Lijuan He, Nuala Del Piccolo, Kalina Hristova *

Department of Materials Science and Engineering, Johns Hopkins University, 3400 North Charles Street, Baltimore, MD 21218, USA

ARTICLE INFO

Article history:
Received 4 December 2013
Received in revised form 28 February 2014
Accepted 1 March 2014
Available online 11 March 2014

Keywords:
Transmembrane domain
Dimerization

ABSTRACT

Here, we study the homodimerization of the transmembrane domain of Neu, as well as an oncogenic mutant (V664E), in vesicles derived from the plasma membrane of mammalian cells. For the characterization, we use a Förster resonance energy transfer (FRET)-based method termed Quantitative Imaging-FRET (QI-FRET), which yields the donor and acceptor concentrations in addition to the FRET efficiencies in individual plasma membrane-derived vesicles. Our results demonstrate that both the wild-type and the mutant are 100% dimeric, suggesting that the Neu TM helix dimerizes more efficiently than other RTK TM domains in mammalian membranes. Furthermore, the data suggest that the V664E mutation causes a very small, but statistically significant change in dimer structure. This article is part of a Special Issue entitled: Interfacially Active Peptides and Proteins. Guest Editors: William C. Wimley and Kalina Hristova.

1. Introduction

Receptor tyrosine kinases (RTKs) are membrane proteins involved in the transduction of biochemical signals across the plasma membrane [1]. Their activation initiates signaling cascades within the cell that are critical for the regulation of cell growth, proliferation, differentiation, and motility [2,3]. An RTK consists of an N-terminal extracellular domain, a single pass transmembrane domain, and a C-terminal tyrosine kinase domain. In order to become active, RTKs must undergo dimerization in the membrane, which leads to the cross-phosphorylation of their tyrosine kinase domains and initiates downstream signaling cascades [4]. RTK dimerization is modulated by binding of ligands to the RTK extracellular domains, with the notable exception of the ErbB2 (HER/Neu) receptor, which has no activating ligand and exhibits ligand-independent activation [5–7]. Not surprisingly, this receptor has been implicated in the progression of many cancers [8–10].

The transmembrane (TM) domains of RTKs have been shown to play an important thermodynamic role in the activation process [11,12]. In particular, isolated TM domains have been shown to dimerize in liposomes and in bacterial membranes, implying that the interactions between the TM domains help stabilize the full-length dimers [13–19]. Importantly, the TM domains have been shown to interact even in the presence of the large RTK extracellular domains [20]. RTK TM domains have been further proposed to play an important structural role in activation, as the interactions between them ensure that the kinase domains achieve the correct orientation and positioning [11,12,21–23]. Since ErbB2/Neu does not require a ligand for activation, its TM domain has been intensively researched with the hope that these studies will reveal some of the physical requirements for ErbB2/Neu activation. Yet, despite many studies, there is no consensus about the contribution of the TM domains of HER2/Neu to dimerization, as different experimental studies have produced very divergent results [24–29].

One of the first discovered RTK TM domain pathogenic mutations is the oncogenic V664E mutation in rat HER/Neu/ErbB2 [30,31]. This mutation has been shown to increase the activation of Neu [32]. Furthermore, it has been suggested that Glu664 stabilizes the mutant TM domain dimer via hydrogen bonding, and this dimer stabilization is sufficient to overactivate the receptor [33,34]. This hypothesis has been investigated in the literature, but while some studies have provided support for it [35,36], others have directly contradicted it [27].

To date, quantitative characterization of the dimerization of the Neu TM domain and related TM sequences has been performed in detergents [24–26], known to be imperfect mimics of biological membranes, or in bacterial membranes [26–29], known to be thinner than the mammalian membrane. Characterization of Neu dimerization in mammalian membranes, on the other hand, has relied predominantly on chemical cross-linking [36,37], a technique that cannot give information about the relative abundance of monomers and dimers due to the limited (and generally unknown) yield of the cross-linking reaction. Here, we present the first measurement of Neu TM domain

☆ This article is part of a Special Issue entitled: Interfacially Active Peptides and Proteins. Guest Editors: William C. Wimley and Kalina Hristova.

* Corresponding author.
E-mail address: kh@jhu.edu (K. Hristova).

http://dx.doi.org/10.1016/j.bbamem.2014.03.001
0005-2736/

dimerization in plasma membrane vesicles derived from mammalian cells.

2. Materials and methods

2.1. Plasmids

The plasmids encoding for the full-length wild-type Neu and the V664E mutant were a generous gift from D. J. Donoghue at UCSD. The genes encoding the TM sequences of Neu and Neu/V664E were inserted in a pcDNA 3.1(+) vector (Invitrogen, CA) by ligation of the transmembrane PCR products using the HindIII and XbaI restriction sites as described previously [38]. The 15 amino acid linker followed by eYFP was inserted into the pcDNA 3.1+Neu/NeuNT constructs via ligation with the following primers to amplify the linker and eYFP: Forward: 5′-GGC GGT ACC GGA GGA AGT GGC GGA AGT GG-3′. Reverse: 5′-GGC GGC TCT AGA GGG TTA CTT GTA CAG CTC GTC CAT GCC G-3′. The PCR primers added a KpnI restriction site upstream of the linker and an XbaI restriction site downstream. The pcDNA–NeuTM–15aa–eYFP construct was digested with AgeI and XbaI to remove only eYFP leaving the rest of the construct intact. Then mCherry was amplified with the following primers: Forward: 5′-GGC ACC GGT G AGC AAG GGC GAG GAG GAT AAC-3′. Reverse: 5′-GGC GGC TCT AGA GGG TTA CTT GTA CAG CTC GTC CAT GCC G-3′, with AgeI and XbaI inserted upstream and downstream of mCherry. This PCR product was then ligated to create the pcDNA–NeuTM–15aa–mCherry construct.

2.2. Cells and expression

Chinese hamster ovary (CHO) cells were used for all experiments as they do not express ErbB receptors. Cells were seeded in six-well plates at a density of 4×10^4 cells per well and were allowed to grow overnight prior to transfection. CHO cells were transfected using a Fugene HD reagent (Promega) and 2–4 μg of total DNA according to the manufacturer's protocol.

2.3. Vesiculation

Twenty-four hours after transfection, the cells were vesiculated following the established protocol of Scott et al. [39]. This consisted of rinsing the cells twice with a calcium and magnesium supplemented phosphate buffered saline (CMPBS) solution and incubating for 1 h at 37 °C in CMPBS supplemented with formaldehyde (25 mM) and dithiolthreitol (DTT, 0.5 mM). The formaldehyde was quenched with an excess of glycine (0.125 M) [40,41]. We have previously shown that dimerization studies in vesicles produced with this protocol and with an alternative osmotic chloride salt method give identical results [42]. Thus, the formaldehyde/DTT treatment does not perturb membrane protein dimerization and the vesicles produced with this treatment are an adequate model of the plasma membrane.

2.4. Image acquisition

Vesicles were transferred to four-chamber coverglass slides (ThermoScientific, Nunc Lab-Tek II) for imaging. All images were acquired with a Nikon C1 laser scanning confocal microscope. Each vesicle was imaged using three scans: donor, FRET and acceptor. For the FRET and donor scans, a 488 nm excitation source was used. For the acceptor scan, a 543 nm excitation source was used. The donor and FRET images were acquired with 500–530 nm and 565–615 nm filters, respectively, while the acceptor was imaged with a 650 nm long pass filter. All images were taken at a resolution of 512×512 pixels with a pixel dwell time of 1.68 μs, the shortest possible for our set-up. Standard solutions of purified eYFP and mCherry of known concentrations were imaged for calibration purposes, as described in detail previously [40,43,44].

2.5. Image processing

Vesicle images were processed using an in-house Matlab® code that recognized the boundary of each vesicle in the image, verified the vesicle presence in all three scans, and fitted the intensity profile across the membrane with a Gaussian function. The integrals of the profiles are referred to as I_D, I_{FRET}, and I_A for the three scans: donor, FRET, and acceptor, respectively. To correlate intensity to concentration, fluorescent protein solutions of known concentrations were imaged using the same settings as the vesicles. The concentration of the acceptor (C_A) was determined directly using the following relationship:

$$C_A = \frac{I_A}{i_A}. \tag{1}$$

Here I_A is the intensity of the acceptor scan and i_A is the slope of the intensity versus concentration line for the bulk solutions of purified acceptor (mCherry). Next, the sensitized acceptor emission was calculated from the observed FRET intensity (I_{FRET}) by determining the bleed-through coefficients, β_D and β_A, for the donor and acceptor, and correcting for bleed-through in the vesicle images:

$$I_{SEN} = I_{FRET} - \beta_A I_A - \beta_D I_D. \tag{2}$$

The corrected donor concentration ($C_{D,Corr}$) was calculated from the observed donor intensity (I_D), using the gauge factor, G_F, which relates the sensitized emission of the acceptor to the FRET efficiency, and depends on the microscope set-up and the FRET pair:

$$C_{D,Corr} = \frac{G_F I_{SEN} + I_D}{i_D}. \tag{3}$$

FRET for each vesicle was then calculated as follows:

$$E = 1 - \frac{I_D}{G_F I_{SEN} + I_D}. \tag{4}$$

As discussed previously [45], the measured FRET efficiency E is a sum of the FRET that occurs due to specific dimerization, and a second FRET contribution, arising due to donors and acceptors approaching each other by chance within distances of 100 Å or less. This "random proximity" contribution follows the model of Wolber and Hudson [46], which has been experimentally verified [47]. The proximity contribution to FRET, which depends on the acceptor concentration only, is then subtracted from the observed FRET to obtain FRET due to dimerization:

$$E_D = E - E_{proximity}. \tag{5}$$

Within the context of a two-state thermodynamic model of dimerization, where monomers and dimers are in equilibrium, E_D is related to the dimeric fraction, f, according to:

$$f \times \tilde{E} = \frac{E_D}{x_A}. \tag{6}$$

Here x_A is the acceptor fraction, C_A / (C_A + $C_{D,corr}$), and $\tilde{E}$ is the FRET efficiency for a dimer with a donor and an acceptor. The value of $\tilde{E}$ depends on the average distance between the fluorescent proteins in the dimer, r, and therefore, on the structure of the dimer. The value of $\tilde{E}$ is given by the following equation:

$$\tilde{E} = \frac{1}{1 + \left(\frac{r}{R_0}\right)^6}, \tag{7}$$

where R_0 is the Förster radius for the donor–acceptor pair.

3. Results

In these experiments, we used constructs consisting of Neu TM domains (wild-type or mutant), a 15 amino acid linker, and either mCherry or eYFP (a FRET pair) (see Fig. 1). The plasmids were constructed as described in the Materials and methods section. Chinese hamster ovary (CHO) cells were transfected with the genes encoding either the wild-type or mutant Neu TM constructs. After 24 h of growth, plasma membrane derived vesicles were produced as described previously [41,42]. Each vesicle contained the Neu TM constructs from the plasma membrane of one cell, and served as a model system for quantitative characterization of Neu TM domain interactions. A FRET-based method, termed QI-FRET, was used to calculate the FRET efficiency, the donor concentration and the acceptor concentration, for each vesicle [20,43,48]. From these parameters, the dimeric fraction and the total protein concentration were calculated for each vesicle. As total protein concentrations in vesicles varied over an order of magnitude in these experiments, the data were combined to produce a dimerization curve [20,43,48].

Vesicles were produced as described previously [40,43] and were transferred to chambered glass slides for image acquisition. Three images, donor, FRET and acceptor, were acquired for each vesicle as discussed in the Materials and methods section. The intensity observed in the acceptor scan, along with Eq. (1), was used to calculate the acceptor concentration in each vesicle. The sensitized emission intensity, (I_{SEN}), was calculated from the observed FRET scan intensity (I_{FRET}) and the bleed-through coefficients using Eq. (2). Once the sensitized emission intensity was determined, the corrected donor intensity was obtained using the gauge factor (G_F) [44]. The concentration of donors was then calculated according to Eq. (3). Finally, the FRET efficiency was calculated for each vesicle according to Eq. (4) and is shown in Fig. 2A with blue symbols for the wild-type and open red symbols for the mutant.

Each data point in Fig. 2A corresponds to a single vesicle, and shows the FRET efficiency for a vesicle versus the acceptor concentration in the same vesicle. The black solid line is generated using the model of Wolber and Hudson [46], while accounting for the size of the fluorescent proteins, and shows the expected FRET due to the random approach of donors and acceptors within distances of 100 Å or less. The data points fall well above this solid line, demonstrating specific interactions between the TM domains in these experiments.

Next, the FRET efficiency in each vesicle that is due to specific interactions was determined using Eq. (5). Given that we already know the acceptor fraction (x_A) in each vesicle, the dimeric fraction multiplied by $\tilde{E}$ is calculated using Eq. (6) for each vesicle. As discussed previously [40], $\tilde{E}$ is the FRET efficiency in a dimer containing one donor and one acceptor, and depends on the average distance between the two fluorophores in the dimer. Since a structural change can alter the distance between the fluorescent proteins, the value of $\tilde{E}$ is a general reporter of dimer structure.

In Fig. 2B, we show the calculated dimeric fraction (f) times $\tilde{E}$ for the wild-type with blue symbols and for the mutant with open red symbols, as a function of total receptor concentration. In Fig. 2C, we average these points within bins, which are of 5×10^{-4} receptors per nm^2 wide. We next performed linear regression analysis on the data, and we tested the null hypothesis that the dimeric fraction (f) times $\tilde{E}$ is uncorrelated

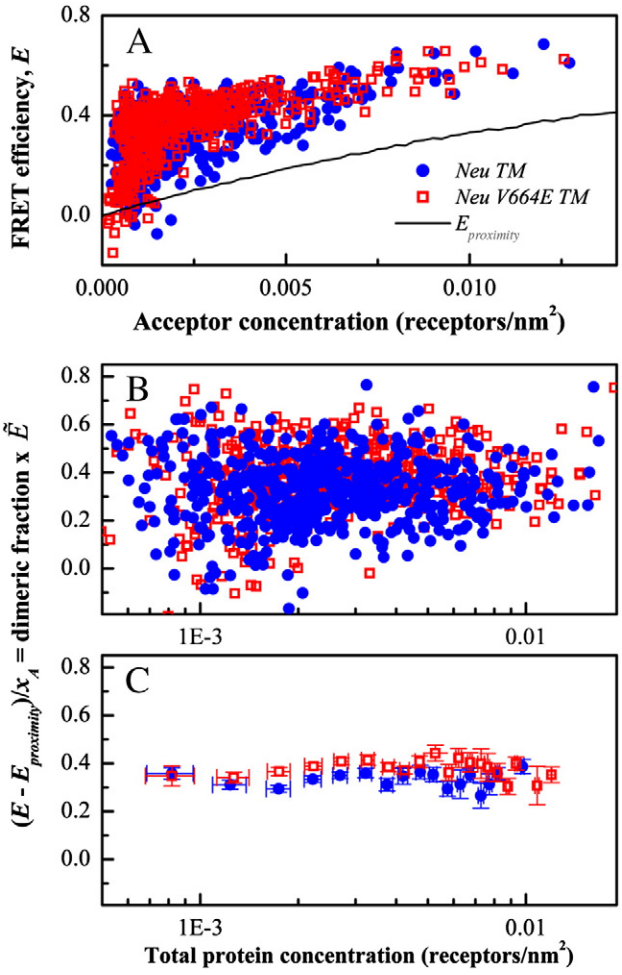

Fig. 2. Measured FRET efficiencies and calculated dimeric fractions for wild-type Neu TM domain and the TM domain with the V664E mutation. Blue circles: wild-type. Open red squares: the V664E mutant. (A) FRET data for wild-type Neu and the V664E mutant constructs as a function of acceptor concentration. Each data point represents a single vesicle, for which the FRET efficiency, the donor concentration, and the acceptor concentration are determined using the QI-FRET method. The solid line shows the so-called called "random FRET" which occurs if there are no specific interactions between the membrane proteins, which is well described by the model of Wolber and Hudson [40]. (B) Dimeric fractions times $\tilde{E}$ for each vesicle, as a function of the protein concentration in the vesicle. (C) Binned dimeric fractions times $\tilde{E}$ as a function of total receptor concentration. Bin size is 5×10^{-4} receptors per nm^2. Each bin contains between three and 85 data points with an average of 22 data points per bin. The averaged data are shown with the standard deviation in the x-direction and with the standard error in the y-direction. The dimeric fractions are independent of protein concentration, indicative of 100% dimer.

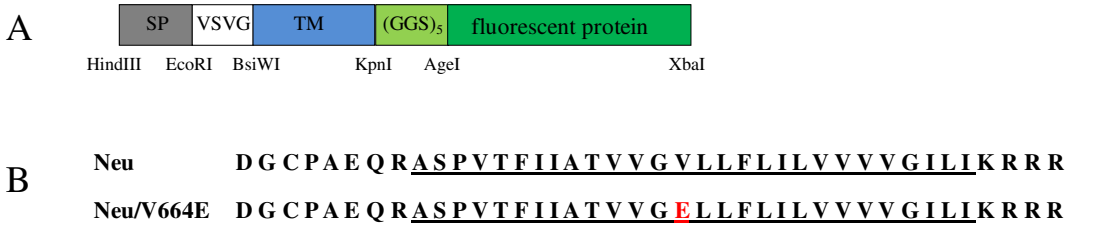

Fig. 1. Proteins used in the study. (A) The genes encoded for the N-terminal signal peptide (SP), a VSV-G tag, the TM domain, a 15 amino acid-long $(GGS)_5$ flexible linker, and the fluorescent proteins (either eYFP or mCherry (a FRET pair)). (B) The amino acid sequences of Neu and Neu/V664E TM domains. The amino acids in the hydrophobic hydrocarbon core — embedded domain are underlined. The mutation is highlighted in red.

with receptor concentration. The calculated p value is >0.2, and it demonstrates that there is no statistically significant correlation. Since $\tilde{E}$ is a constant, this analysis demonstrates that the dimeric fractions do not depend on the concentration, over the protein concentration range that is accessible in our experiments and exceeds an order of magnitude. Within the dimerization model, this plateau corresponds to 100% dimer. Such behavior is observed for both the wild-type and the mutant. Overall, these results demonstrate that both wild-type Neu TM domain and the V664E mutant dimerize in a highly efficient manner, such that the monomeric state is not accessible in the experiments.

The fact that a plateau is reached in the experiments (corresponding to $f = 1$) allows us to determine the values of $\tilde{E}$ for both the wild-type and the mutant. By averaging the data for all concentrations, we obtained $\tilde{E} = 0.33 \pm 0.03$ for the wild-type and $\tilde{E} = 0.38 \pm 0.04$ for the mutant. The difference between these two values is very small, but statistically significant ($p < 0.05$). Next, we calculated the average distance between the proteins in the dimers using Eq. (7). Given that the Förster radius R_0 of the eYFP/mCherry FRET pair is ~53 Å, the distances between the fluorescent proteins were determined as 60 ± 2 Å and 58 ± 2 Å, respectively, for the wild-type and the mutant.

4. Discussion

4.1. Dimerization strength of the Neu TM domain

Previously, the dimerization of wild-type FGFR3 TM domain (as well as wild-type and mutant FGFR3 variants including the EC domain) has been measured in plasma membrane vesicles derived from CHO and HEK 293T cells [43,48]. Such measurements have been performed also for the TM domain of glycophorin A (GpA) [40,41]. The measured dimeric fractions in all these previous cases increased with the total protein concentration in accordance with the law of mass action. In contrast, the data for the Neu TM domain presented here are indicative of 100% dimer, under conditions for which FGFR3 and GpA TM domain dimeric fractions vary between ~50 and ~80% (for the FGFR3 TM domain), and between ~35 and ~70% (for the GpA TM domain). Thus, the Neu TM helix has the highest dimerization propensity in mammalian membranes of all the TM helices that we have encountered in our work. This finding is surprising, since both human and rat ErbB TM domains have been shown to interact very weakly in detergent micelles [19,25,49]. Thus, the environment has a profound effect on the interactions, as previously discussed [50,51], demonstrating that it is critical that RTK TM domain dimerization studies are performed in mammalian membranes.

4.2. Structural insights from the FRET studies

The FRET experiments presented here yield the value of the parameter $\tilde{E}$, the FRET efficiency in a dimer containing one donor and one acceptor. The value of this parameter depends on the distance between the fluorescent proteins in the dimer, and thus $\tilde{E}$ is a reporter of dimer structure. Here we obtain a value of $\tilde{E} = 0.33$ for the Neu dimer, corresponding to a distance of 60 ± 2 Å between the fluorescent proteins.

Based on molecular modeling of wild-type and mutant TM dimers, it has been suggested that the V664E mutation causes a structural change in the Neu TM dimer [52]. Here we demonstrate that $\tilde{E} = 0.38 \pm 0.04$ for the mutant, corresponding to a distance of 58 ± 2 Å between the fluorescent proteins. A chi square analysis of the data reveals a statistically significant change in $\tilde{E}$ due to the mutation, consistent with the hypothesis of a mutation-induced structural change. However, this change is very small, and the exact nature of this change is unknown. We are hopeful that the parameters measured in this work will aid future molecular modeling studies of the Neu TM dimer structure and the effect of the V664E mutation.

Acknowledgements

This work was supported by NIH GM68619 and GM95930. We thank Drs. Daniel Leahy and Eduard Bocharov, and Patrick Byrne, for reading the manuscript prior to submission.

References

[1] J. Schlessinger, Cell signaling by receptor tyrosine kinases, Cell 103 (2000) 211–225.
[2] S.R. Hubbard, W.T. Miller, Receptor tyrosine kinases: mechanisms of activation and signaling, Curr. Opinion Cell Biol. 19 (2007) 117–123.
[3] P. van der Geer, T. Hunter, R.A. Lindberg, Receptor protein–tyrosine kinases and their signal transduction pathways, Annu. Rev. Cell Biol. 10 (1994) 251–337.
[4] M.A. Lemmon, J. Schlessinger, Cell signaling by receptor tyrosine kinases, Cell 141 (2010) 1117–1134.
[5] B. Linggi, G. Carpenter, ErbB receptors: new insights on mechanisms and biology, Trends Cell Biol. 16 (2006) 649–656.
[6] A.W. Burgess, H.S. Cho, C. Eigenbrot, K.M. Ferguson, T.P.J. Garrett, D.J. Leahy, M.A. Lemmon, M.X. Sliwkowski, C.W. Ward, S. Yokoyama, An open-and-shut case? Recent insights into the activation of EGF/ErbB receptors, Mol. Cell 12 (2003) 541–552.
[7] H.S. Cho, K. Mason, K.X. Ramyar, A.M. Stanley, S.B. Gabelli, D.W. Denney, D.J. Leahy, Structure of the extracellular region of HER2 alone and in complex with the Herceptin Fab, Nature 421 (2003) 756–760.
[8] D. Harari, Y. Yarden, Molecular mechanisms underlying ErbB2/HER2 action in breast cancer, Oncogene 19 (2000) 6102–6114.
[9] M.D. Marmor, K.B. Skaria, Y. Yarden, Signal transduction and oncogenesis by ErbB/HER receptors, Int. J. Radiat. Oncol. Biol. Phys. 58 (2004) 903–913.
[10] J. Drevs, M. Medinger, C. Schmidt-Gerbach, R. Weber, C. Unger, Receptor tyrosine kinases: the main targets for new anticancer therapy, Curr. Drug Targets 4 (2003) 113–121.
[11] E. Li, K. Hristova, Role of receptor tyrosine kinase transmembrane domains in cell signaling and human pathologies, Biochemistry 45 (2006) 6241–6251.
[12] E. Li, K. Hristova, Receptor tyrosine kinase transmembrane domains: function, dimer structure, and dimerization energetics, Cell Adhes. Migr. 4 (2010) 249–254.
[13] C. Finger, C. Escher, D. Schneider, The single transmembrane domains of human receptor tyrosine kinases encode self-interactions, Sci. Signal. 2 (2009).
[14] E.O. Artemenko, N.S. Egorova, A.S. Arseniev, A.V. Feofanov, Transmembrane domain of EphA1 receptor forms dimers in membrane-like environment, Biochim. Biophys. Acta 1778 (2008) 2361–2367.
[15] E. Li, M. You, K. Hristova, SDS-PAGE and FRET suggest weak interactions between FGFR3 TM domains in the absence of extracellular domains and ligands, Biochemistry 44 (2005) 352–360.
[16] E. Li, M. You, K. Hristova, FGFR3 dimer stabilization due to a single amino acid pathogenic mutation, J. Mol. Biol. 356 (2006) 600–612.
[17] M. You, E. Li, K. Hristova, The achondroplasia mutation does not alter the dimerization energetics of FGFR3 transmembrane domain, Biochemistry 45 (2006) 5551–5556.
[18] M. You, J. Spangler, E. Li, X. Han, P. Ghosh, K. Hristova, Effect of pathogenic cysteine mutations on FGFR3 transmembrane domain dimerization in detergents and lipid bilayers, Biochemistry 46 (2007) 11039–11046.
[19] L. Chen, M. Merzlyakov, T. Cohen, Y. Shai, K. Hristova, Energetics of ErbB1 transmembrane domain dimerization in lipid bilayers, Biophys. J. 96 (2009) 4622–4630.
[20] S. Sarabipour, K. Hristova, FGFR3 transmembrane domain interactions persist in the presence of its extracellular domain, Biophys. J. 105 (2013) 165–171.
[21] C.A. Bell, J.A. Tynan, K.C. Hart, A.N. Meyer, S.C. Robertson, D.J. Donoghue, Rotational coupling of the transmembrane and kinase domains of the Neu receptor tyrosine kinase, Mol. Biol. Cell 11 (2000) 3589–3599.
[22] L. He, K. Hristova, Physical–chemical principles underlying RTK activation, and their implications for human disease, Biochim. Biophys. Acta 1818 (2012) 995–1005.
[23] N.F. Endres, R. Das, A.W. Smith, A. Arkhipov, E. Kovacs, Y.J. Huang, J.G. Pelton, Y.B. Shan, D.E. Shaw, D.E. Wemmer, J.T. Groves, J. Kuriyan, Conformational coupling across the plasma membrane in activation of the EGF receptor, Cell 152 (2013) 543–556.
[24] J.P. Duneau, A.P. Vegh, J.N. Sturgis, A dimerization hierarchy in the transmembrane domains of the HER receptor family, Biochemistry 46 (2007) 2010–2019.
[25] A.M. Stanley, K.G. Fleming, The transmembrane domains of ErbB receptors do not dimerize strongly in micelles, J. Mol. Biol. 347 (2005) 759–772.
[26] A.J. Beevers, A. Nash, M. Salazar-Cancino, D.J. Scott, R. Notman, A.M. Dixon, Effects of the oncogenic V(664)E mutation on membrane insertion, structure, and sequence-dependent interactions of the Neu transmembrane domain in micelles and model membranes: an integrated biophysical and simulation study, Biochemistry 51 (2012) 2558–2568.
[27] J.M. Mendrola, M.B. Berger, M.C. King, M.A. Lemmon, The single transmembrane domains of ErbB receptors self-associate in cell membranes, J. Biol. Chem. 277 (2002) 4704–4712.
[28] C. Escher, F. Cymer, D. Schneider, Two GxxxG-like motifs facilitate promiscuous interactions of the human ErbB transmembrane domains, J. Mol. Biol. 389 (2009) 10–16.
[29] D. Gerber, N. Sal-Man, Y. Shai, Two motifs within a transmembrane domain, one for homodimerization and the other for heterodimerization, J. Biol. Chem. 279 (2004) 21177–21182.
[30] C.I. Bargmann, M.C. Hung, R.A. Weinberg, Multiple independent activations of the Neu oncogene by a point mutation altering the transmembrane domain of P185, Cell 45 (1986) 649–657.

[31] C.I. Bargmann, R.A. Weinberg, Oncogenic activation of the Neu-encoded receptor protein by point mutation and deletion, EMBO J. 7 (1988) 2043–2052.
[32] M. Miloso, M. Mazzotti, W.C. Vass, L. Beguinot, SHC and GRB-2 are constitutively activated by an epidermal growth factor receptor with a point mutation in the transmembrane domain, J. Biol. Chem. 270 (1995) 19557–19562.
[33] S.O. Smith, C.S. Smith, B.J. Bormann, Strong hydrogen bonding interactions involving a buried glutamic acid in the transmembrane sequence of the neu/erbB-2 receptor, Nat. Struct. Biol. 3 (1996) 252–258.
[34] S.O. Smith, C. Smith, S. Shekar, O. Peersen, M. Ziliox, S. Aimoto, Transmembrane interactions in the activation of the Neu receptor tyrosine kinase, Biochemistry 41 (2002) 9321–9332.
[35] D.B. Weiner, J. Liu, J.A. Cohen, W.V. Williams, M.I. Greene, A point mutation in the neu oncogene mimics ligand induction of receptor aggregation, Nature 339 (1989) 230–231.
[36] L. He, K. Hristova, Pathogenic activation of receptor tyrosine kinases in mammalian membranes, J. Mol. Biol. 384 (2008) 1130–1142.
[37] S.J. Weiner, P.A. Kollman, D.A. Case, U.C. Singh, C. Ghio, G. Alagona, S. Profeta, P. Weiner, A new force field for molecular mechanical simulation of nucleic acids and proteins, J. Am. Chem. Soc. 106 (1984) 765–784.
[38] L.J. He, N. Shobnam, K. Hristova, Specific inhibition of a pathogenic receptor tyrosine kinase by its transmembrane domain, Biochim. Biophys. Acta Biomembr. 1808 (2011) 253–259.
[39] R.E. Scott, Plasma membrane vesiculation: a new technique for isolation of plasma membrane, Science 194 (1976) 743–745.
[40] L. Chen, L. Novicky, M. Merzlyakov, T. Hristov, K. Hristova, Measuring the energetics of membrane protein dimerization in mammalian membranes, J. Am. Chem. Soc. 132 (2010) 3628–3635.
[41] S. Sarabipour, K. Hristova, Glycophorin A transmembrane domain dimerization in plasma membrane vesicles derived from CHO, HEK 293T, and A431 cells, Biochim. Biophys. Acta 1828 (2013) 1829–1833.
[42] N. Del Piccolo, J. Placone, L. He, S.C. Agudelo, K. Hristova, Production of plasma membrane vesicles with chloride salts and their utility as a cell membrane mimetic for biophysical characterization of membrane protein interactions, Anal. Chem. 84 (2012) 8650–8655.
[43] L. Chen, J. Placone, L. Novicky, K. Hristova, The extracellular domain of fibroblast growth factor receptor 3 inhibits ligand-independent dimerization, Sci. Signal. 3 (2010) ra86.
[44] E. Li, J. Placone, M. Merzlyakov, K. Hristova, Quantitative measurements of protein interactions in a crowded cellular environment, Anal. Chem. 80 (2008) 5976–5985.
[45] M. Merzlyakov, K. Hristova, Forster resonance energy transfer measurements of transmembrane helix dimerization energetics, Methods Enzymol. Fluoresc. Spectrosc. 450 (2008) 107–127.
[46] P.K. Wolber, B.S. Hudson, An analytic solution to the Förster energy transfer problem in two dimensions, Biophys. J. 28 (1979) 197–210.
[47] Y.O. Posokhov, M. Merzlyakov, K. Hristova, A.S. Ladokhin, A simple “proximity” correction for Forster resonance energy transfer efficiency determination in membranes using lifetime measurements, Anal. Biochem. 380 (2008) 134–136.
[48] J. Placone, K. Hristova, Direct assessment of the effect of the Gly380Arg achondroplasia mutation on FGFR3 dimerization using quantitative imaging FRET, PLoS ONE 7 (2012) e46678.
[49] L.J. He, A.R. Hoffmann, C. Serrano, K. Hristova, W.C. Wimley, High-throughput selection of transmembrane sequences that enhance receptor tyrosine kinase activation, J. Mol. Biol. 412 (2011) 43–54.
[50] F. Cymer, A. Veerappan, D. Schneider, Transmembrane helix–helix interactions are modulated by the sequence context and by lipid bilayer properties, Biochim. Biophys. Acta Biomembr. 1818 (2012) 963–973.
[51] E. Li, W.C. Wimley, K. Hristova, Transmembrane helix dimerization: beyond the search for sequence motifs, Biochim. Biophys. Acta Biomembr. 1818 (2012) 183–193.
[52] S.J. Fleishman, J. Schlessinger, N. Ben-Tal, A putative molecular-activation switch in the transmembrane domain of erbB2, Proc. Natl. Acad. Sci. U. S. A. 99 (2002) 15937–15940.